University of Huddersfield Repository

Shoghi, K., Barrans, Simon and Rao, H.V.

Plastic deformation in flat-section band clamps

Original Citation

This version is available at http://eprints.hud.ac.uk/id/eprint/1345/

http://eprints.hud.ac.uk/

Plastic deformation in flat-section band clamps

K Shoghi*, **S M Barrans,** and **H V Rao**
Department of Mechanical Engineering, University of Huddersfield, Huddersfield, UK

Abstract: Previous work on the elastic deformation of flat-section band clamps has been extended to account for plastic deformation of the band material. Both finite element analysis using a multilinear plastic model and a classical approach using a continuous plastic equation are reported. The excellent agreement between the results of these two approaches provides a high level of confidence in the models. The finite element approach was found to be extremely time consuming owing to the combination of changing contact non-linearity and material non-linearity. The classical approach provided a much faster solution method when used with the iteration schemes proposed here. The classical method of analysis was used to determine the response to a range of conditions. This analysis showed that there might be some advantage in driving flat-section band clamps into the partially plastic state. In this state the coefficient of friction has far less impact on the variation in circumferential stress, and hence radial clamping force, around the band.

Keywords: stress, flat-section band clamp, contact with friction, rigid cylinder, plastic deformation, material non-linearity, finite element model, coefficient of friction

1 INTRODUCTION

Flat band clamps are widely used for connecting flexible tubes or hoses to comparatively rigid ducts or pipes. They consist of a simple circular band of material carrying two trunnion straps, as shown in Fig. 1. The band is tightened using a T-bolt connecting the two trunnions. The purpose of the flat-section band clamp is to provide a pressure seal between the components by supplying the required radial pressure on the flexible component of the joint. Band clamps have been available for many years, and developments to try to ensure that the radial load is evenly distributed have taken place over a similar period. These include overlapping the ends of the band, as suggested by Jones [1], and including inserts in the area under the T-bolt, as advocated by Schaub [2]. Recently, Shoghi *et al.* [3] have described the elastic behaviour of such clamps and demonstrated that, owing to frictional effects, it is unlikely that the radial load will be evenly distributed.

In demanding applications and during maintenance, a band clamp may well be tightened beyond the original design load. Typically, ultimate failure will occur in the T-bolt rather than the flat band (see reference [4]). However, before this failure point is reached, it is likely that, owing to the non-uniform stress distribution around the clamp, plastic deformation will occur in some areas. While there will be no visible effect from this deformation, it could well compromise operational performance. There is therefore a need to understand this partially plastic state.

Although finite element methods could be employed to find the relationship between stress and displacement beyond the yield point, the band-clamp problem is highly non-linear owing to the contact condition. Adding material non-linearity to the problem makes obtaining a converged solution difficult and time consuming. Consequently, the present paper sets out a theory applicable to a wide range of flat-section band clamps taking account of material non-linearity.

2 DEVELOPMENT OF MODELS

The hoses joined by flat-section clamps are typically made from flexible materials, while the ducts or

---

**Corresponding author: Borgwarner Turbo Systems, Roysdale Way, Euroway Industrial Estate, Bradford, West Yorkshire BD4 6SE, UK.*
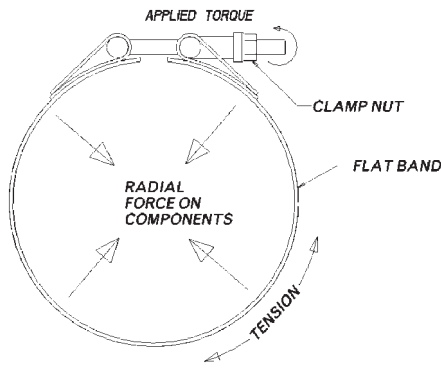
Fig. 1 Flat-section band clamp components

pipes to which they are being connected to are comparatively rigid. In the analyses presented here, the components being joined are assumed to be rigid. The flexible nature of hoses, ducts, etc., may be taken into account by making the final closed radius of the band, R (see Fig. 2), equal to the compressed outer radius of such flexible components.

2.1 Theoretical stress–displacement relationship

As with the elastic analysis previously presented [3], it is assumed that stress within the band is uniform both across the width and through the thickness. The analysis of the band can then be divided into two parts, an elastic portion governed by Hooke's law and a non-linear region. The stress distribution
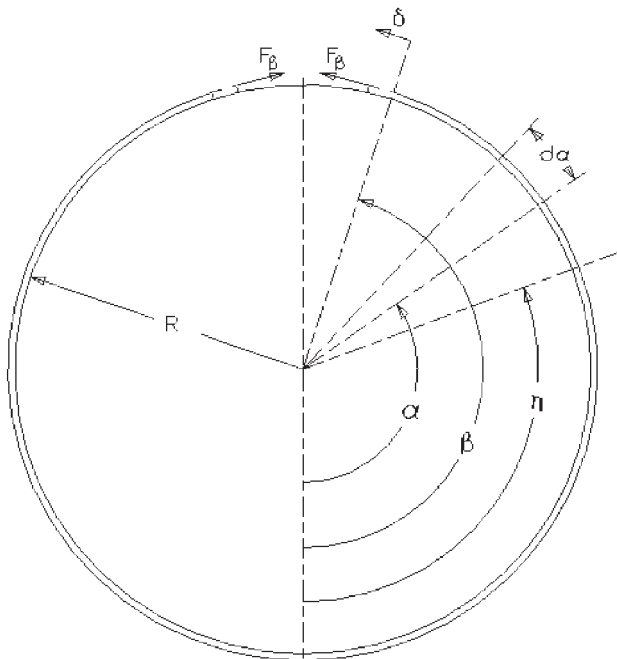
in the elastic region will be as given by Shoghi *et al.* [3].

The relationship between the clamping load, F_β, and hoop stress, σ_α, at angle α (see Fig. 2) is given by Shoghi *et al.* [3] as

$$\sigma_\alpha = \frac{F_\beta \exp[\mu(\alpha - \beta)]}{wt} \tag{1}$$

This relationship was established by considering force equilibrium and is therefore applicable to both the elastic and plastic regions. However, F_β is difficult to control or measure. It is therefore necessary to relate the hoop stress to the more readily controllable circumferential displacement, δ.

From equation (1) it can be seen that the largest stress will occur at the gap. Hence, yielding and plastic deformation will initiate at this point and gradually propagate towards the back of the clamp ($\alpha = 0$). The boundary between the elastic and plastic regions will occur at some angle, η. At this boundary the value of stress σ_α given by equation (1) will equal the yield stress, σ_Y. Hence, from equation (1)

$$\sigma_Y = \frac{F_\beta \exp[\mu(\eta - \beta)]}{wt} \tag{2}$$

The boundary angle, η, is therefore given by

$$\eta = \beta - \frac{1}{\mu} \ln\left(\frac{F_\beta}{wt\sigma_Y}\right) \tag{3}$$

The elastic circumferential deformation of the band was found previously by Shoghi *et al.* [3]. For an elastic region $0 < \alpha < \eta$, this deformation will be

$$\delta_E = \frac{RF_\beta}{Ewt} \int_0^\eta \exp[\mu(\alpha - \beta)] \, d\alpha$$

Hence

$$\delta_E = \frac{RF_\beta[\exp(\mu\eta) - 1]}{Ewt\mu \exp(\mu\beta)} \tag{4}$$

The relationship between stress and displacement, δ_p, for the non-linear region should be determined taking into account the non-linearity due to the material. From Fig. 3 the strain is given by

$$\varepsilon = \frac{d\delta_p}{R \, d\alpha} \tag{5}$$

where $d\delta_p$ is the extension of a small segment, $R \, d\alpha$, of the band.

Fig. 2 Elastic–plastic analysis of the flat section band clamp
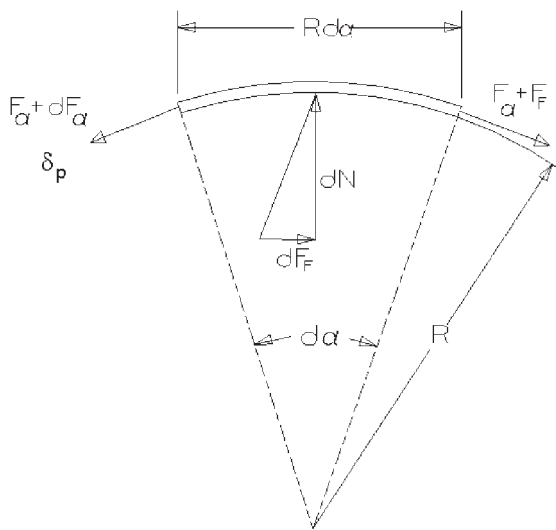
Fig. 3 Deformation of a band segment

As Hill [5] describes, there are a number of models available to simulate the non-linear behaviour of metals. One of the simplest of these is the power law

$$\sigma = C + A\varepsilon^n \tag{6}$$

The difficulty in using this model for the whole stress–strain curve is that it tends to underestimate stress at low levels of strain and overestimates stress for larger strains. However, the slightly simpler model

$$\sigma = A\varepsilon^n \tag{7}$$

can give quite a reasonable fit to the plastic region alone. In the implementation here, this equation is used in combination with a linear model for the elastic region.

In order to determine the constants A and n, two points on the stress–strain curve are selected such that the strain values between these two points covers the required range of strain. A pair of simultaneous equations for A and n is thereby generated.

Combining equations (5) and (7) allows the stress at angle α within the plastic region to be related to the plastic deformation at that point

$$\left(\frac{\sigma_\alpha}{A}\right)^{1/n} = \frac{\mathrm{d}\delta_\mathrm{p}}{R\,\mathrm{d}\alpha} \tag{8}$$

Combining equations (1) and (8) gives

$$\mathrm{d}\delta_\mathrm{p} = \left[\frac{F_\beta \exp[\mu(\alpha - \beta]}{Awt}\right]^{1/n} R\,\mathrm{d}\alpha$$

Hence

$$\delta_\mathrm{p} = R\left(\frac{F_\beta}{Awt\exp(\mu\beta)}\right)^{1/n} \cdot \int_\eta^\beta \exp\left(\frac{\mu\alpha}{n}\right) \mathrm{d}\alpha \tag{9}$$

Thus, the value of the plastic displacement, δ_p, can be expressed as

$$\delta_\mathrm{p} = \frac{nR}{\mu}\left(\frac{F_\beta}{Awt}\right)^{1/n}\left\{1 - \exp\left[\left(\frac{\mu}{n}\right)(\eta - \beta)\right]\right\} \tag{10}$$

and the total displacement, δ, is given by

$$\delta = \delta_\mathrm{E} + \delta_\mathrm{p}$$

Hence

$$\delta = \frac{R}{\mu}\left(\frac{F_\beta[\exp(\mu\eta) - 1]}{Ewt\exp(\mu\beta)} + n\left(\frac{F_\beta}{Awt}\right)^{1/n}\right.$$
$$\left. \times \left\{1 - \exp\left[\left(\frac{\mu}{n}\right)(\eta - \beta)\right]\right\}\right) \tag{11}$$

2.2 Method for calculating the stress distribution in the band for a given displacement

Calculation of the stress distribution in the band at a given displacement using the elastic–plastic model is complex and requires an iterative procedure. A suitable procedure is given by the flow chart shown in Fig. 4.

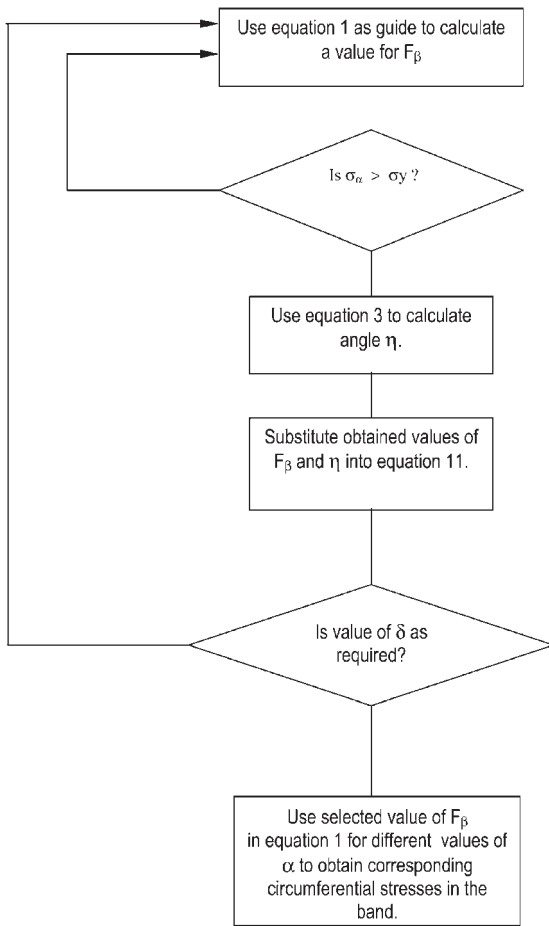## 2.3 Angular displacement around the band with plasticity

In order to determine the displacement at different angular locations on the band it is necessary to establish an expression for the incremental plastic displacement, δ_ip, at angle α_p. Using equation (9) gives

$$\delta_\mathrm{ip} = R\left[\frac{F_\beta \exp(-\mu\beta)}{Awt}\right]^{1/n} \cdot \int_\eta^{\alpha_\mathrm{p}} \exp\left(\frac{\mu\alpha}{n}\right) \mathrm{d}\alpha$$

Hence, the incremental plastic deformation is given by

$$\delta_\mathrm{ip} = R\left[\frac{F_\beta \exp(-\mu\beta)}{Awt}\right]^{1/n}$$
$$\times \left\{\frac{n}{\mu}\left[\exp\left(\frac{\mu\alpha_\mathrm{p}}{n}\right) - \exp\left(\frac{\mu\eta}{n}\right)\right]\right\} \tag{12}$$

This is valid for $\alpha_\mathrm{p} > \eta$.

Fig. 4 Method used to calculate stress distribution in the band

The total incremental displacement, δ_T, at angle α_p is given by

$$\delta_T = \delta_{ip} + \delta_E \tag{13}$$

2.4 Finite element analysis

A model of the flat-section band interacting with a rigid cylinder was constructed using three-dimensional elements with a quadratic interpolation polynomial. The reason for using a quadratic element was to ensure that the elements took up the curved shape of the band clamp and cylinder. This criterion is best explained by imagining a bicycle chain wrapped around a rigid cylinder. The straight chain links will prevent full contact between the chain and the cylinder, and hence reduce the contact area. A similar effect would have been observed in the case here if linear elements had been used. Ciabattoni (D. Ciabattoni, 2000, personal communication) confirmed that, in the finite element code used for this problem, contact is detected at the Gaussian integration points. This

allows contact pressure to be correctly calculated by integrating over the face of the element. Hence, the usual difficulty associated with contact and higher-order elements is avoided.

Surface-to-surface elements were used for this analysis. These elements are well suited for this type of application where a significant amount of sliding and friction is involved. These contact elements can be used with both lower and higher-order continuum elements within the simulated model.

Symmetry of the flat-section band about two planes was used to reduce the size of the model and to allow constraints to be applied on the planes of symmetry shown in Fig. 5. The clamp was loaded by applying a pressure to the end face of the clamp equivalent to the circumferential force applied by the T-bolt. The band was also constrained along the edge of the section, as shown, to eliminate potential rigid body displacement.

2.5 Modelling material non-linearity

In the development of the theoretical model of the band clamp described in section 2.1, a non-linear material model of a form similar to those described by Hill [5] was utilized. One difficulty in using this type of model is in matching it to the observed yield stress and the elastic behaviour. For materials that do not exhibit a distinct yield point, a percentage proof stress is normally used to indicate the onset of plastic strain and replaces the yield stress in many design formulae. In this work a 0.2 per cent proof stress, $\sigma_{0.2}$, has been used. For the analysis described here, the 'yield stress' must occur at the intersection of the linear elastic region and the plastic stress–strain curve approximated by equation (7).
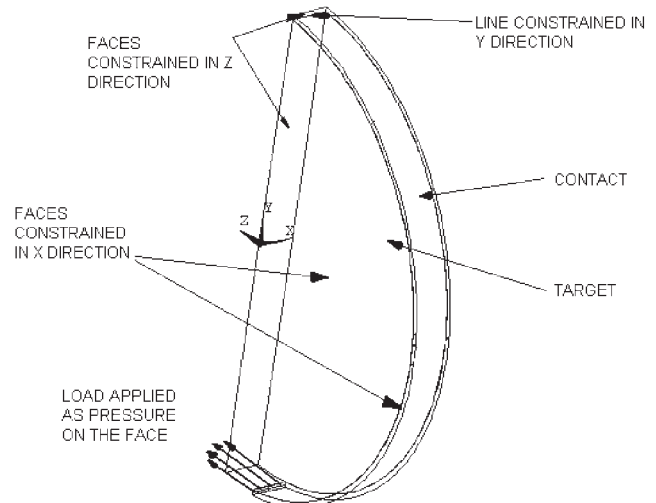
Fig. 5 Finite element model

Hence, at the yield point

$$\frac{\sigma_Y}{E} = \left(\frac{\sigma_Y}{A}\right)^{1/n}$$

Solving for yield stress from the above equation gives

$$\sigma_Y = \left(\frac{E^n}{A}\right)^{(1/n-1)} \tag{14}$$

Using equation (14), the modelled value of yield stress, σ_Y, can be calculated.

Modelling the material behaviour now involves the standard process of determining the Young's modulus (see, for example, reference [6]), establishing a suitable fit within the plastic region, and matching these two models at a sensible yield point. The iterative process illustrated by the flow chart shown in Fig. 6 was used to achieve this.
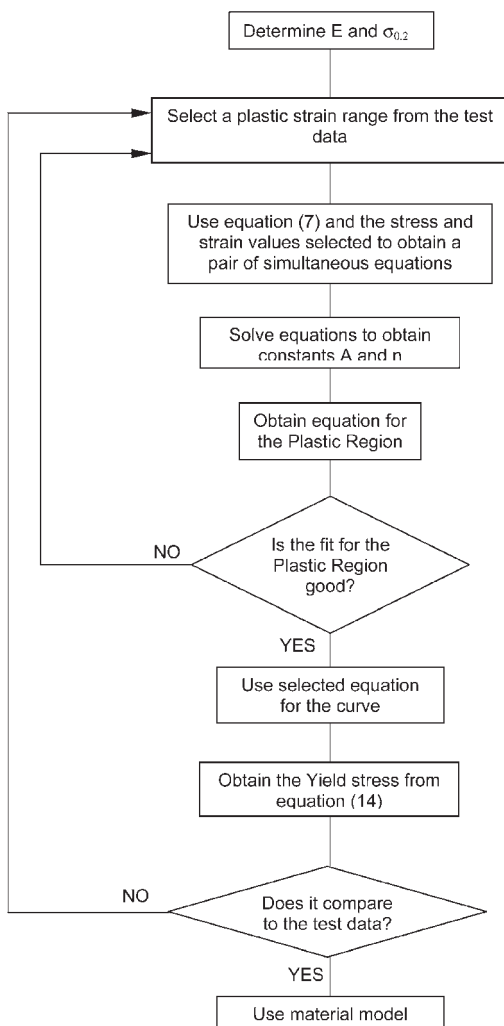

Fig. 6 Method used to determine the theoretical material model

Within the finite element software a multilinear isotropic hardening model was used rather than the more complex single curve in the theoretical model. The non-linear material behaviour may be defined using the data obtained from a tensile test as a sequence of up to 20 stress–strain data points within the plastic region. Realistically, it is usually faster and more robust to use a simplified multilinear model with five or six slopes.

It is important that the slope (σ_1/ε_1) for the first point of entry corresponds to the elastic modulus given in the material properties. Here, σ_1 and ε_1 refer to the stress and corresponding strain values for the first point. No part of the curve segment may have a slope larger than the elastic modulus. Negatives slopes are not recommended and could cause convergence problems. The software assumes elastic–perfectly plastic behaviour for the values past the end-point defined by the table.

3 MODEL COMPARISON

3.1 Geometry and material data

To investigate the performance of the finite element and theoretical models, they were used to investigate the behaviour of a sample band clamp. The dimensions of this clamp are given in Table 1.

The stress–strain curve shown in Fig. 7 was determined by carrying out a tensile test on a sample of band material. The process shown in Fig. 6 was used to determine the material model shown in Fig. 7 and Table 2.

To define the material model for the finite element simulation, the initial yield stress shown in Table 2 was used along with an additional four points taken from the tensile test data. These points along with the multilinear material model are also shown in Fig. 7. The elastic modulus used in the finite element model was 227 kN/mm² and Poisson's ratio was 0.29.

3.2 Discussion of the results for the finite element model

The finite element model described in section 2.4 was analysed with an end load of 16.1 kN applied as a pressure load to the cross-sectional area near the open gap. The maximum corresponding von

Table 1 Properties of the flat-section band clamp

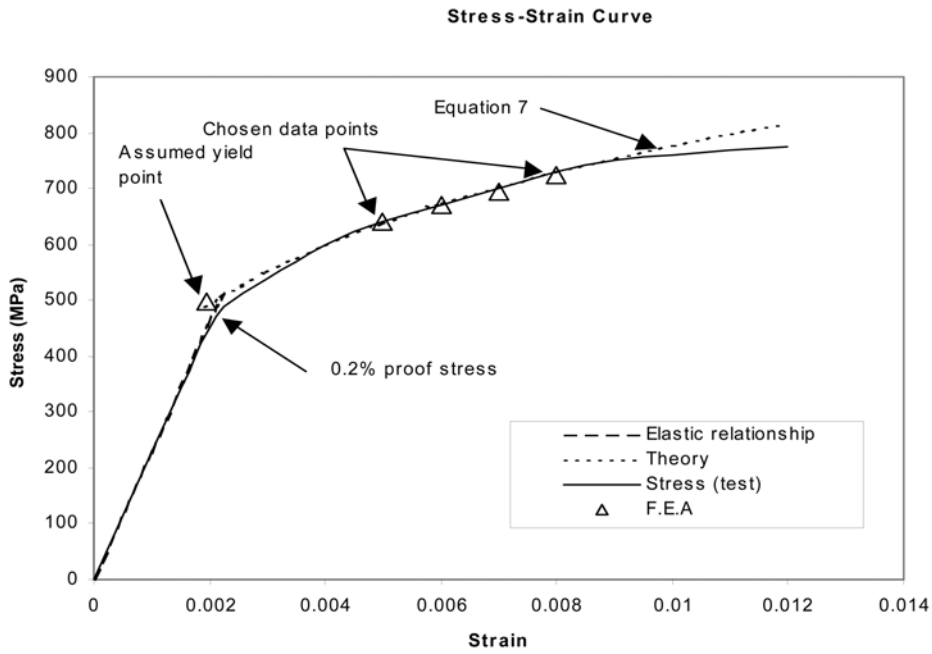|	
Width, w	18.85 mm
Band thickness, t	1.22 mm
Initial radius, R	59.5 mm
Subtended angle of half the band, β	162°

Stress-Strain Curve

Fig. 7 Stress–strain curve

Mises stress in the flat-section band is 704.379 MPa and occurs near the gap. A coefficient of friction, μ, of 0.3 was used for this model. The stress plot is shown in Fig. 8. As a quality check, the circumferential stresses predicted by the finite element model at the end of the band were compared with the applied stress of 700 MPa. The stress from the model was 682 MPa, indicating an error due to stress field approximation of less than 3 per cent. The difference between the von Mises equivalent stress and the circumferential stress is due to the presence of the direct radial stress due to contact and shear stresses resulting from friction between the band and the flange.

In the finite element model it is not straightforward to identify the boundary between the elastic and plastic regions accurately. This is defined as angle η. This position can be shown in the finite element analysis results by setting the yield stress as the minimum stress to plot, as shown in Fig. 8. The value of angle η can then be determined from the position of the nodes on or close to this boundary.

3.3 Comparison of results

Having identified the boundary between the elastic and plastic regions, the plastic displacement can be

located on the model. This is shown in Fig. 9 along with the results predicted by the theory presented in section 2 and the results of the linear analysis of the same problem as presented by Shoghi [3]. The excellent correlation between these models is immediately evident. The effect of material non-linearity is also clearly shown. As expected, in the elastic region the elastic and elastic–plastic models

Fig. 8 Plastic stress plot

Table 2 Material properties of the flat-section band clamp

Constant, A	2.86×10^9
Constant, n	0.283
Elastic modulus, E	227 kN/mm^2
Yield stress, σ_Y	525 N/mm^2

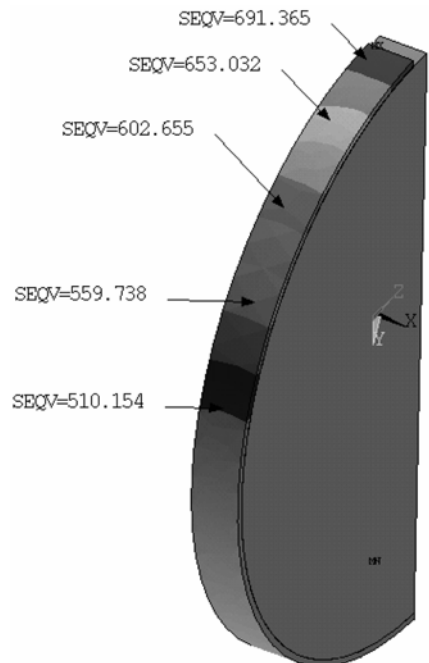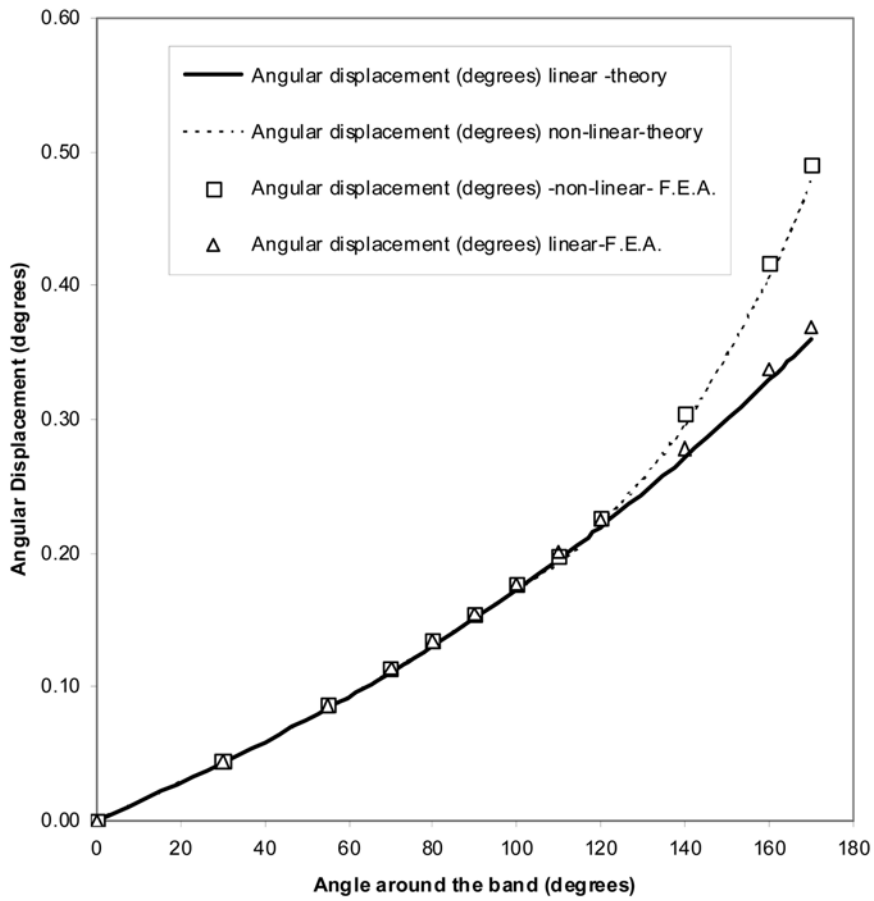**Fig. 9** Angular displacement for elastic and plastic regions
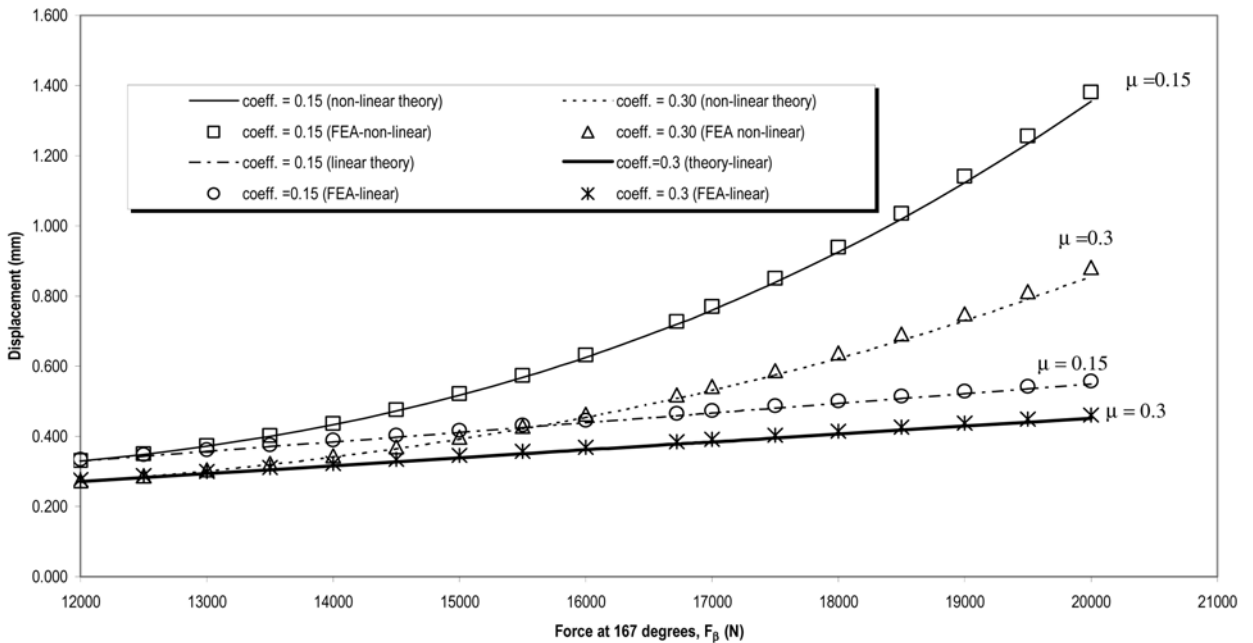

Fig. 10 Effect of material non-linearity on total displacement

Table 3 Summary of the results for contact with friction and material non-linearity

Coefficient of friction, μ	0.15	0.15	0.3	0.3	0.5	0.5
Method of calculation	FEA	Theory	FEA	Theory	FEA	Theory
Displacement, δ (mm)	0.728	0.716	0.518	0.505	0.368	0.357
Difference (%)	1.64	1.64	2.5	2.5	3	3
Elastic–plastic boundary angle, η (deg)	34	34.2	103	102	127	125
Difference (%)	0.97	0.97	1.45	1.45	1.57	1.57

give identical results. However, in the plastic region the non-linear model produces much larger displacements.

The relationship between force and total displacement with two different coefficients of friction is shown in Fig. 10. The graph demonstrates good correlation between the theory developed in section 2 and the finite element model with material non-linearity. It is worth noting that, as the force is increased, the correlation between theory and finite element model has slightly deteriorated. This is due to the limits inherent in the material model defined by equation (7) and Table 2. This limitation can also be seen in Fig. 7 where, for higher strains, the stress prediction deviates from the test results. However, corrections could be made by obtaining a different range for equation (7) to cater for higher loads. This can be achieved by changing the constants A and n.

A summary of the results from the finite element and theoretical models for a clamping load $F_\beta = 16 \, \text{kN}$ is given in Table 3. The correlation between the results obtained using equations (3) and (11) and the finite element method is excellent. Table 3 shows a larger difference for a coefficient of friction of 0.3 compared with 0.15. This is due to

stress concentration within a smaller plastic region near the gap and can be corrected by refining the mesh density in this area.

Verification of non-linear results is more complex than verification of linear results, because, by their nature, non-linear results tend to be harder to predict. However, the excellent correlation between the theoretical and finite element results presented here provides confidence in both calculation methods.

4 NON-LINEAR EFFECTS AND BAND PERFORMANCE

4.1 Relationship between stress and displacement

In order to examine the effect of the non-linear material model, the graph of hoop stress against displacement shown in Fig. 11 for the flat-section band clamp analysed in section 3 was plotted. Equations (1), (4), and (11) were used to predict the stress for the angles $\alpha = 162$, $\alpha = 90$, and $\alpha = 0$ for the band described in Tables 1 and 2. A coefficient of friction of 0.15 was assumed. It should be noted
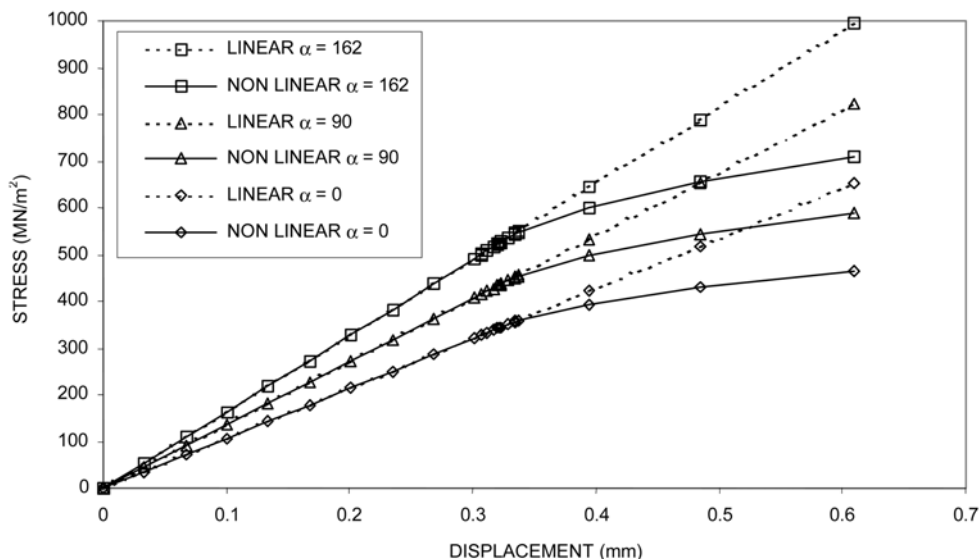
Fig. 11 Hoop stress at angle α for linear and non-linear material model
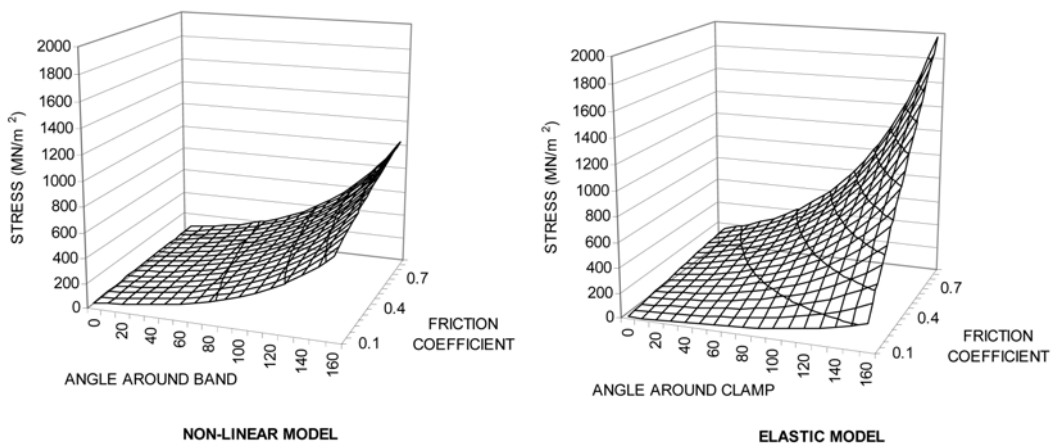
Fig. 12 Stress distribution around the clamp

here that the displacement and stress due to initial bending of the band clamp has been omitted for clarity. It can be seen that, while the band clamp is fully elastic, the graph remains linear. A change in the slope of the graph shows the start of yielding. As the elastic–plastic interface, η, moves around the band clamp towards $\alpha = 0°$, the displacement increases rapidly for small increases in hoop stress. It can be observed here that, since the total circumferential displacement is a function of the strain around the whole clamp, yielding at one point in the clamp makes the stress–displacement relationship non-linear at all other points in the clamp. Hence, the non-linearity observed is due to both the material non-linearity and the development of the plastic region.

4.2 Stress distribution

Using the procedure described in the flow chart, given in Fig. 4, the graph of the hoop stress at different levels of friction with the non-linear material model was determined at different values of angle around the band for a total displacement value $\delta_T = 0.6$ mm. This level of displacement generated plastic deformation in the clamp across the full range of friction coefficients. All other properties of the flat-section band were as given in Tables 1 and 2. The same calculation was carried out using the purely elastic model of band behaviour previously presented by Shoghi *et al.* [3]. The results of these analyses are shown in Fig. 12. As expected, the elastic model predicts higher stresses in order to generate the same level of displacement. It is also observed that, at low levels of friction, the plastic model gives a larger variation in stress around the clamp. However, at higher levels of friction this situation is reversed, with the non-linear model giving more even stresses. These variations in stress are

important since the radial clamping force is directly proportional to the circumferential stress.

It can also be seen that the non-linear model predicts a much smaller effect due to variations in the coefficient of friction. This illustrates a possible advantage in driving this type of clamp into the plastic region since the coefficient of friction is probably the least controllable variable in this type of application and can vary substantially depending on the material being clamped.

5 CONCLUSIONS

A theoretical model has been developed to predict the deformation in flat-section band clamps where the material has been loaded into the plastic region. A method for determining the elastic–plastic stress distribution for an applied displacement has also been proposed. This classical approach has been validated against the results of finite element analyses of the problem, with differences between the two approaches being less than 3 per cent. The larger differences occur at higher levels of friction owing to the difficulty in modelling the larger concentration of stress towards the band T-bolt.

The circumferential stress, and hence the radial clamping load, in partially plastic band clamps shows significantly less variation due to changes in the coefficient of friction than the equivalent elastic band. However, at lower coefficients of friction the partially plastic band exhibits more stress variation around the clamp.

REFERENCES

1 **Jones, W. G.** Hose clamp for thin wall tubes. US Pat. 2852832, 1958.
2 **Schaub, E.** T-bolt hose clamp. US Pat. 6584654, 2003.

3 Shoghi, K., Rao, H. V., and **Barrans, S. M.** Stress in flat section band clamp. *Proc. Instn Mech. Engrs, Part C: J. Mechanical Engineering Science*, 2003, **217**, 821–830.

4 Shoghi, K. Stress and strain analysis of V-section band clamps. PhD thesis, University of Huddersfield, 2004.

5 Hill, R. *The Mathematical Theory of Plasticity*, 1950, pp. 12–13 (Oxford University Press, London).

6 Dean, G. D., Loveday, M. S., Cooper, P. M., Read, B. E., Roebuck, B., and **Morrel, R.** Aspects of modulus measurement. In *Materials Metrology and Standards for Standard Performance* (Eds B. G. Dyson, M. S. Loveday, and M. G. Gee), 1995, Ch. 8, pp. 150–209 (Chapman and Hall, London).

APPENDIX

Notation

A constant
E elastic modulus (GPa)
F_f friction force (N)
F_α circumferential force at angle α (N)
F_β clamp force (second stage) (N)

n constant
R radius of the band (m)
t thickness of the band (m)
W width of the band (m)

α contact angle for the band (rad)
α_p contact angle for the band for the plastic region (rad)
β subtended angle of half the flat band (rad)
δ total displacement (m)
δ_E elastic displacement (m)
δ_{ip} incremental plastic displacement (m)
δ_p plastic displacement (m)
δ_T total incremental displacement at angle α_p (m)
ε strain
η elastic–plastic boundary angle (rad)
θ_T total angular displacement (rad)
μ coefficient of friction between the band and the rigid cylinder
σ_Y yield stress (MPa)
σ_α hoop stress at angle α (MPa)
$\sigma_{0.2}$ 0.2 per cent proof stress (MPa)